Transactions, SMiRT-26
Berlin/Potsdam, Germany, July 10-15, 2022
Division II

XFEM Analysis of Non-uniform Fatigue Crack Growth Crossing Interface in Cladded Plate

Masaki Nagai[1], Toshio Nagashima[2], Naoki Miura[3] and Tomoki Shinko[4]

[1] Research Scientist, Central Research Institute of Electric Power Industry, Yokosuka, Kanagawa, JAPAN (nagai@criepi.denken.or.jp)
[2] Professor, Sophia University, Tokyo, JAPAN
[3] Distinguished Research Scientist, Central Research Institute of Electric Power Industry, Yokosuka, Kanagawa, JAPAN
[4] Research Scientist, Central Research Institute of Electric Power Industry, Yokosuka, Kanagawa, JAPAN

ABSTRACT

In light water reactor plants, inner surface of reactor pressure vessel made from low-alloy steel is cladded by austenitic stainless steel to improve the corrosion resistance of the vessel. In the evaluations of the crack propagation at the J-welding portions of bottom mounted instrumentations in pressurized water reactors or at the build-up welding portions of control rod drive housings in boiling water reactors, it is assumed that crack may propagate crossing the dissimilar materials interface between the base metal of low-alloy steel and the stainless steel cladding. Crack growth rate of the cladding is predicted to be captured by that of the base metal because the thickness of the cladding is very thin compared with that of the base metal. In this study, fatigue crack growth analyses of cladded plate under cyclic loading were carried out using XFEM, which can model crack independently of finite elements.

INTRODUCTION

In light water reactor plants, inner surface of reactor pressure vessel (RPV) made of low-alloy steel is cladded by austenitic stainless steel to improve the corrosion resistance of the RPV. In a structural integrity assessment of cladded components such as RPV with a postulated crack, the JSME Rules on Fitness-for-Service for Nuclear Power Plants (JSME FFS) (2019) shows a method to deal conservatively with the cladding, that is assumed not to have a loadbearing capacity, as follows: A crack that penetrates the cladding and extends into the base metal shall be evaluated based on the total crack depth in both the cladding and the base metal. In the evaluations of the crack propagation at the J-welding portions of bottom mounted instrumentations in pressurized water reactors or at the build-up welding portions of control rod drive housings in boiling water reactors, it is assumed that crack may propagate crossing dissimilar materials interface between base metal of low-alloy steel and cladding of austenitic stainless steel. It is predicted that crack growth rate of the cladding is captured by that of the base metal because the thickness of the cladding is very thin compared with that of the base metal. In the previous study (2019), fatigue crack growth test of a cladded plate was performed to observe the crack propagation behavior crossing dissimilar materials interface. The cladded plate was fabricated by deposing austenitic stainless steel onto carbon steel, whose fatigue crack growth rate is close to that of low-alloy steel. Consequently, non-uniform crack propagation that the crack in the base metal propagates differently from that in the cladding was observed. In order to evaluate such non-uniform crack propagation, numerical method is crucial. Conventional finite element method (FEM), which is used originally to perform the crack propagation analysis, requires a time-consuming mesh generation process for specific crack configuration. The consideration of a propagating crack is further accentuated because the crack propagation behavior along the crack front is implicitly

affected by the distribution of the crack driving force along the crack front. The extended finite element method (XFEM) (1999) can approximate the discontinuous displacement field near the crack front independently of the finite element mesh, and therefore XFEM can simulate crack propagation without remeshing.

In this study, fatigue crack growth analyses of the cladded plate under cyclic loading were carried out using XFEM to evaluate the non-uniform crack propagation behavior.

EXTENDED FINITE ELEMENT METHOD

In this study, we used the XFEM program developed by one of the authors (2020). An analysis domain is defined in the Cartesian coordinates (x, y, z), and a planar crack is assumed to be in any plane parallel to the x-y plane. In XFEM, the approximate displacement, $\mathbf{u}^h$, at any position, $\mathbf{x}$, near the crack is expressed as follows:

$$\boldsymbol{u}^h(\boldsymbol{x}) = \sum_{I=1}^{p} N_I(\boldsymbol{x})\boldsymbol{u}_I + \sum_{I\in \boldsymbol{J}} N_I(\boldsymbol{x})H(z)\,\boldsymbol{b}_I \tag{1}$$

Where N_I is the interpolation function used in the formulation of conventional FEM, $\mathbf{J}$ denotes the node sets considering the Heaviside function $H(\mathbf{x})$ representing the discontinuity of displacement near the crack, and $\mathbf{u}_I$, and $\mathbf{b}_I$ denote the vectors of freedoms assigned to each node.

PROCEDURE FOR FATIGUE CRACK PROPAGATION

Fatigue crack propagation analysis is carried out by calculating the stress intensity factor at each evaluation point on the crack front and determining the amount of crack extension based on the following Paris' law:

$$\frac{da}{dN} = C(\Delta K)^m \tag{2}$$

where a , N and ΔK are crack depth, cycle number and stress intensity factor range at the evaluation point, respectively, and C and m are material properties. The unit of da/dN is mm/cycle and that of ΔK is MPa $m^{1/2}$. The crack is supposed to extend to the direction normal to the crack front. The crack propagation and subsequent change of the crack shape are simulated by the integration of the extension at all evaluation points along the crack front. As the crack grows, the distances between each evaluation point on the crack front become uneven due to different extension at each point. In the present study, as shown in Figure 1, the coordinates of evaluation points are approximated by cubic Bezier curve and then they are moved on the lines so that they are arranged in equal intervals at every time the crack propagates. On the boundary such as the interface or the intersection of the crack front and the free surface, the evaluation point is determined by linear extrapolation of coordinates of the nearest two evaluation points. If discrepancy of the crack extension is occurred on the interface, their points are moved on the intermediate between them as shown in Figure2.

In this analysis, we calculate the J-integral, which is equal to the energy release rate in linear elastic body, at all evaluation points. The stress intensity factor distributions along the crack front are obtained through the relationship between the stress intensity factor and the energy release rate. In order to evaluate the J-integral for three-dimensional problems, some computational techniques (1977, 1987) have been developed. In the finite element models used in XFEM analysis, the geometries of the crack front do not always match the faces and edges of the mesh. Therefore, the virtual crack extension method, which is used in conjunction with conventional FEM analysis, cannot be applied to calculate the J-integral. In the present study, the domain integral method can be applied to evaluate the J-integral in conjunction with XFEM.

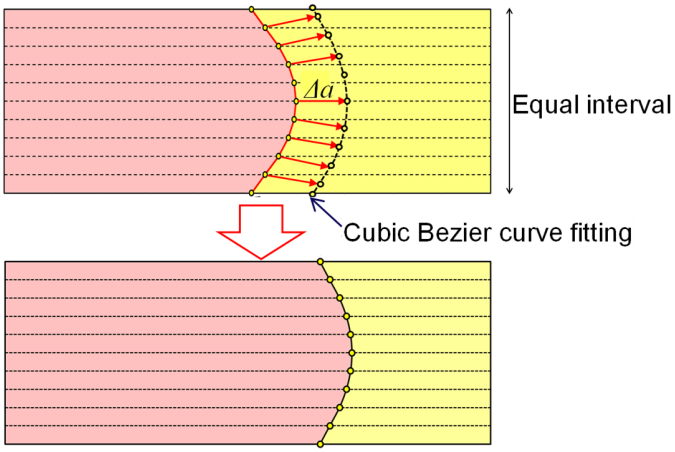

Figure 1 Rearrangement of evaluation points with crack propagation

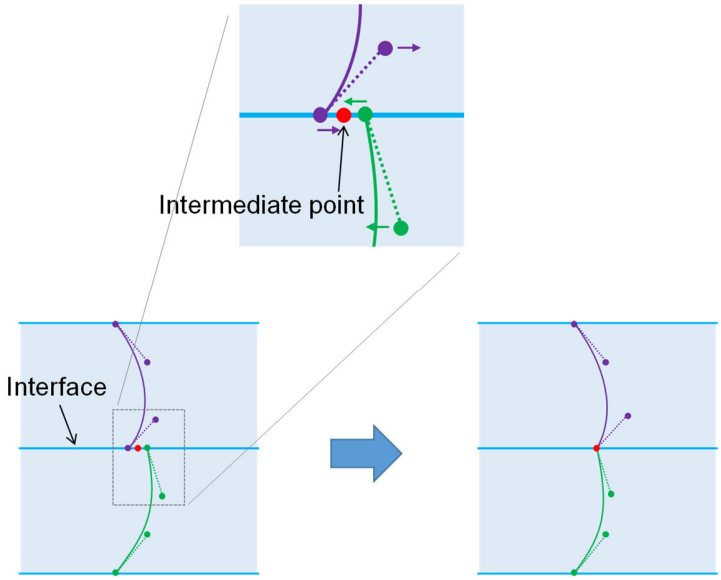

Figure 2 Determination of evaluation point on interface between base meal and cladding

We define the Cartesian local coordinate (x_1, x_2, x_3) at the evaluation point on the crack front as shown in Figure 3. The x_3 axis is perpendicular to the crack plane, and the x_1 and x_2 axes lie on the crack plane, and are normal and tangent to the crack front, respectively. The volume integral form of the J-integral in three-dimensional problems can be represented as follows:

$$J = \frac{\int_V \left[\left(\sigma_{ij}\frac{\partial u_j}{\partial x_1} - w\delta_{1i}\right)\frac{\partial q}{\partial x_i}\right] dV}{\int_{L_c} \eta ds} \tag{3}$$

where L_c is a small segment of the crack front that undergoes a virtual crack advance on the crack plane, η is the virtual crack advance that takes the unity at the evaluation point and vanishes at endpoints of the segment L_c, and σ_{ij}, u_j, and w are the stress, displacement, and strain energy density, respectively. V is a rectangular parallelepiped region defined in local coordinate (x_1, x_2, x_3) and centered on the evaluation point. q is the weight function that takes the unity at the evaluation point and vanishes at the surface of the volume V. The weight function q is expressed by the following equation:

$$q(x_1, x_2, x_3) = \left(1 - \frac{2x_1}{L_1}\right)\left(1 - \frac{2x_2}{L_2}\right)\left(1 - \frac{2x_3}{L_3}\right) \quad (4)$$

where L_1, L_2, and L_3 are the lengths of the edges of the rectangular parallelepiped in the x_1, x_2, and x_3 directions, respectively.

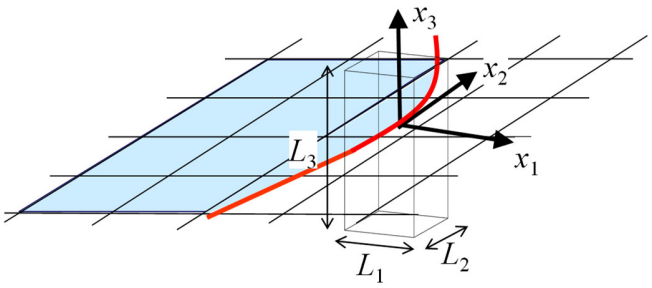

Figure 3 Volume for domain integral to compute J-integral in three-dimensional crack

ANALYSIS MODEL

We analyzed the compact tension specimen composed of JIS SM490A carbon steel and Type 308 stainless steel with the same dimensions as the specimen used in the previous study (2019). The total thickness of the model is 25.4 mm as shown in Figure 4, and the thickness of the cladding of Type 308 stainless steel is 5 mm. An initial crack-front was modeled to match with the shape of the initial beachmark introduced in the test. The material properties are shown in Table1, in which C and m used in the Paris' law were determined through a series of fatigue crack growth tests for each of the base metal and the cladding (see Figure 5). The cladding portion was assumed to be a transverse isotropic material because many columnar crystal grains were observed in the macroscopic test of the cladding. The elastic stiffnesses of the cladding were measured by the Electro-Magnetic Acoustic Resonance method. On the other hand, Young's modulus and Poisson's ratio of the base metal were determined by the ultrasonic method. As loading condition, the maximum and minimum loads were set to be 23 kN and 2.3 kN, respectively, so that the average of ΔK for evaluation points on the initial crack-front could be approximately 22 MPa $m^{1/2}$. Because of the symmetry of the geometry, one half of the specimen was modelled. As shown in Figure 6, eight-node hexahedral elements were used in the finite element model. The smallest size of elements, which lie on the crack-plane, around the crack front was 0.25 mm. In fatigue crack growth analyses, the maximum crack extension Δa is controlled to be 0.25 mm every time the crack propagates.

Table 1 Mechanical properties of materials used in the study.

	Proof strength, MPa	Young's modulus, GPa	Poisson's ratio	Paris' law	
				C	m
SM490 carbon steel (Base metal)	339	$E = 210.98$	$\nu = 0.28$	2.56×10^{-10}	3.98
Type 308 stainless steel (Cladding)	221	$E_1 = E_2 = 182.52$, $E_3 = 121.25$	$\nu_{12} = 0.166$, $\nu_{13} = \nu_{23} = 0.515$	2.60×10^{-10}	4.09

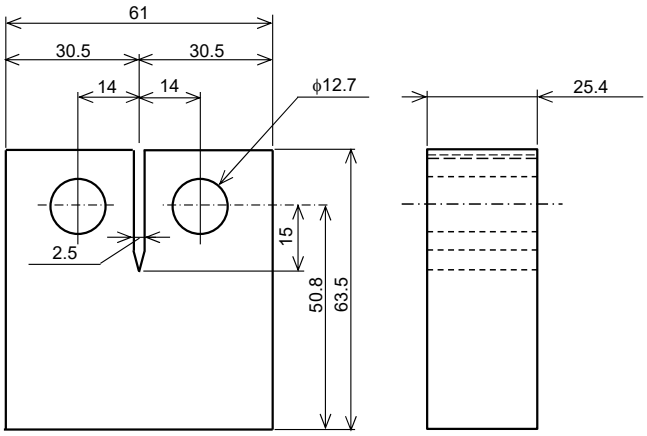

Figure 4 Geometry of compact tension specimen

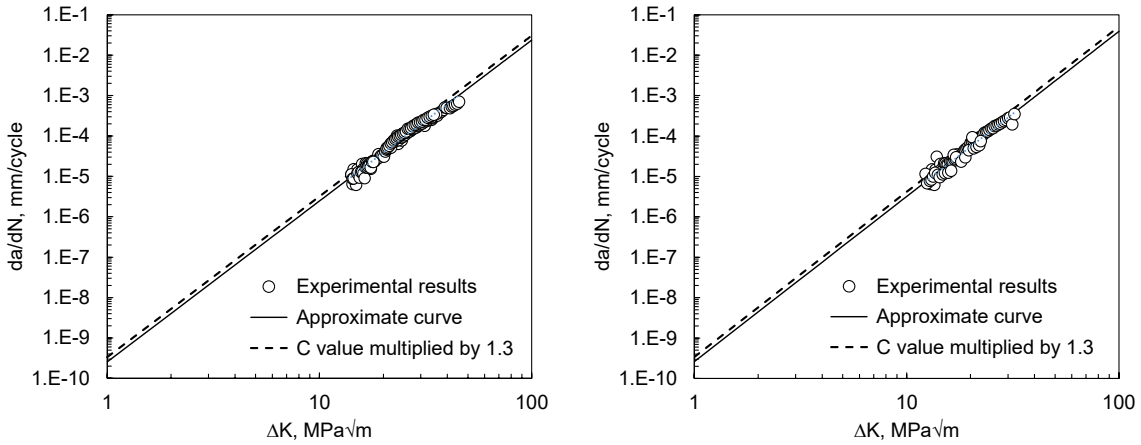

(a) Base metal (SM490A carbon steel) (b) Cladding (Type 308 stainless steel)

Figure 5 Relationship between da/dN and ΔK for base metal and cladding

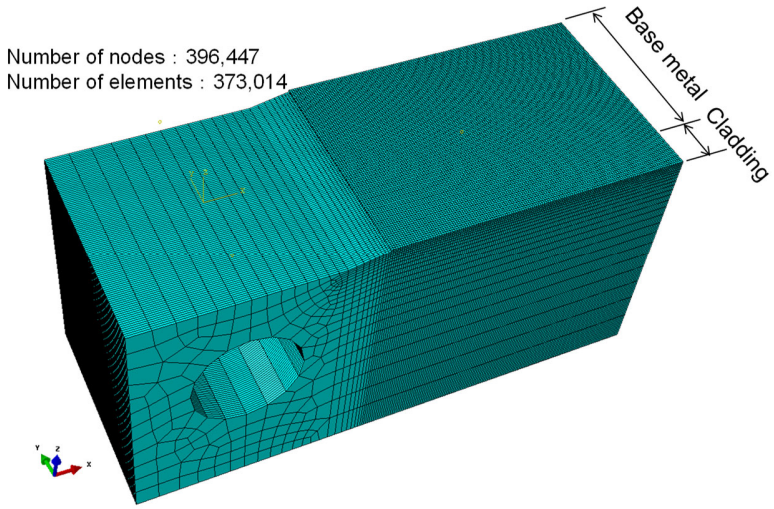

Figure 6 Finite element mesh used in analysis (Half model)

RESULTS AND DISCUSSION

The validity of analysis results was examined by comparing the calculated crack front shapes and the amounts of crack extension with experimental results. The fatigue crack growth test was conducted subjected to sinusoidal cyclic load with the frequency of 1 Hz, and the specimen was exposed to air environment at room temperature. Figure 7 depicts the fracture surface of the cladded specimen with some beachmarks after the test. The white dashed line indicates the maximum crack extension when small scale yielding condition seems to be satisfied. From the transition of experimental beachmarks, non-uniform crack propagation behavior can be observed. In particular, the crack propagates faster in the base metal than in the cladding under the condition of small scale yielding. When the small scale yielding condition is no longer satisfied, the crack growth rate of the cladding is partially high near the interface but is still low in other part including the free surface.

Figure 7 Transition of crack front shapes with crack propagation

In Figure 8, typical crack fronts obtained by XFEM are compared with the beachmarks introduced in the experiment. In the figure, red figure indicates the number of cycles and the beachmarks obtained by the experiment and blue figure stands for the number of cycles and the crack front obtained by XFEM. It should be noted that the fatigue crack propagation analysis was conducted based on Paris' law even though the small scale yielding condition is not satisfied. Transitions of the crack extension from the notch-tip shown in Figure 4 on both side surfaces of the specimen with cycle number are shown in Figure 9. From these figures, although the calculated crack front shapes do not completely match beachmarks, non-uniform crack propagation behavior is simulated by XFEM. However, the calculated crack growth is slow compared with the experimental results. This may be attributed to statistical variability of the measured fatigue crack growth rate by the experiment. Then, the XFEM analysis was carried out when material properties C in Paris' law of both the base metal and the cladding set to be 1.3 times as large as the original values. We do not have statistical data on the variation of C so far, however, JSME FFS (2019) states that 2.7 C corresponds to twice of the standard deviation in the fatigue crack growth for austenitic stainless steels in PWR environment. If the same estimate is applied, 1.3C is considered to be approximately equal to the standard deviation. The obtained results are presented in Figures 10 and 11. These figures indicate that the

cyclic numbers of typical crack front in XFEM are in good agreement with those of corresponding beachmarks.

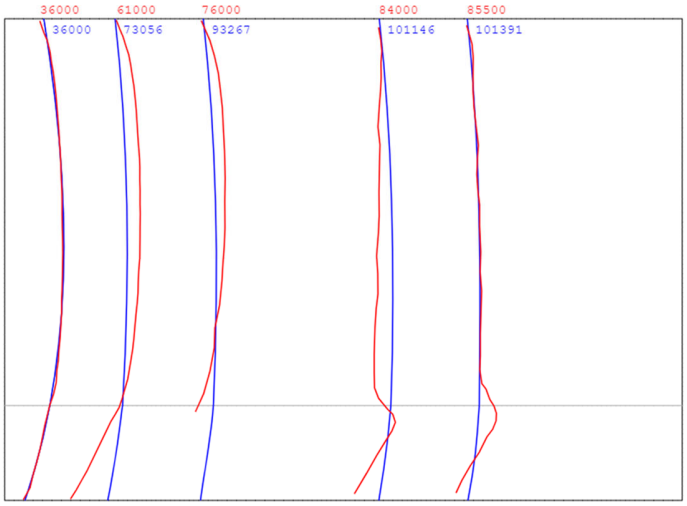

Figure 8 Comparison of calculated crack front shapes with experimental beachmarks
(Red figure indicates the number of cycles and the beachmaks obtained by the experiment and blue figure stands for the number of cycles and the crack fronts obtained by XFEM.)

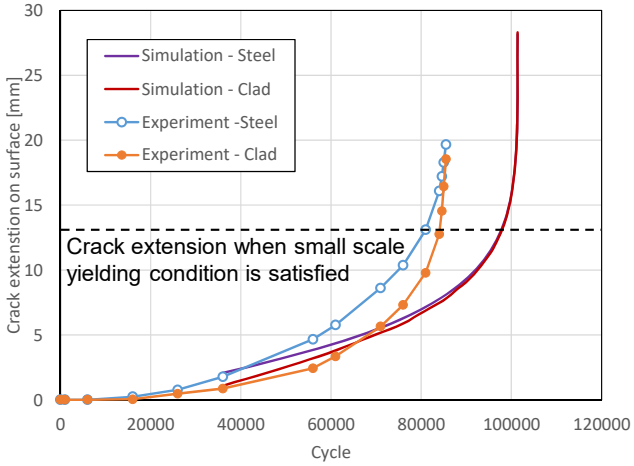

Figure 9 Transitions of crack extension on both side surfaces of cladded specimen with cycle number

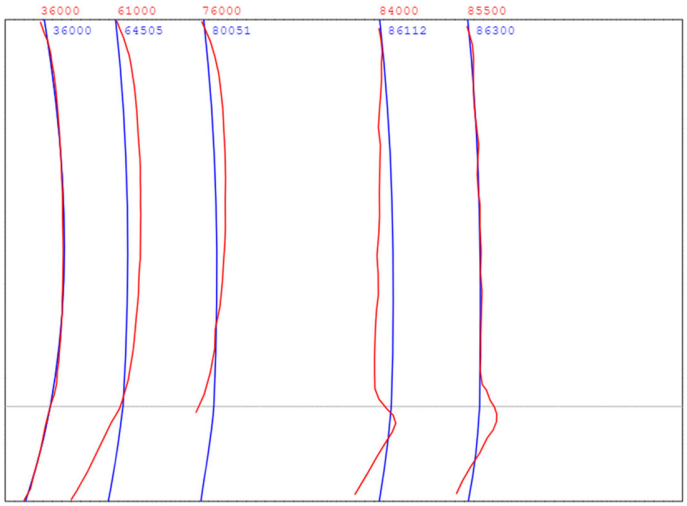

Figure 10 Comparison of calculated crack front shapes with experimental beachmarks
(XFEM analysis was performed with the C values which set to be 1.3 times as large as the original values. Red figure indicates the number of cycles and the beachmarks obtained by the experiment and blue figure stands for the number of cycles and the crack fronts obtained by XFEM.)

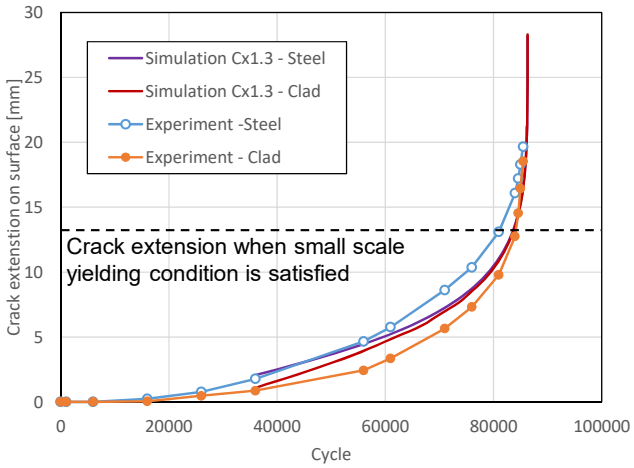

Figure 11 Transitions of crack extension on both side surfaces of cladded specimen with cycle number
(XFEM analysis was performed with the C values which set to be 1.3 times as large as the original values.)

CONCLUSION

In this study, fatigue crack growth analyses of the cladded plate under cyclic loading were carried out using XFEM, which can model crack independently of finite elements. The validity of analysis results was examined by comparing the calculated crack front shapes and the amounts of crack extension with experimental results. Consequently, the transition tendency of the crack extension with cycle number obtained by XFEM is in well agreement with that by the experiment. Furthermore, non-uniform crack propagation that the crack in the base metal propagates differently from that in the cladding was simulated.

REFERENCES

Japan Society of Mechanical Engineers (2019). "Code for Nuclear Power Generation Facilities – Rules on Fitness-for-Service for Nuclear Power Plants -", JSME S NA1-2019.

Moes, N., Dolbow, J. and Belytschko, T., "A finite element method for crack growth without remeshing", International Journal for Numerical Methods in Engineering, Vol. 46 (1999), pp. 131-150.

Moran, B. and Shih, C. F., "A general treatment of crack tip contour integrals," International Journal of Fracture, Vol. 35 (1987), pp. 295-310.

Nagai, M., Miura, N. and Nagashima, T., "Non-uniform fatigue crack propagation test crossing interface in cladded plate", Proceedings of 25th Conference on Structural Mechanics in Reactor Technology (SMiRT25), 2019.

Nagashima, T., "Three-dimensional crack analyses under thermal stress field by XFEM using only the Heaviside step function", Mechanical Engineering Journal, Vol. 7, Issue 4, Pages 20-00098, 2020.

Parks, D. M., "The virtual crack extension method for nonlinear material behavior," Computational Methods in Applied Mechanics and Engineering, Vol. 12 (1977), pp. 353-364.